Cell Reports, Volume *28*

Supplemental Information

Wnd/DLK Is a Critical Target of FMRP Responsible for Neurodevelopmental and Behavior Defects in the *Drosophila* Model of Fragile X Syndrome

Alexandra Russo and Aaron DiAntonio

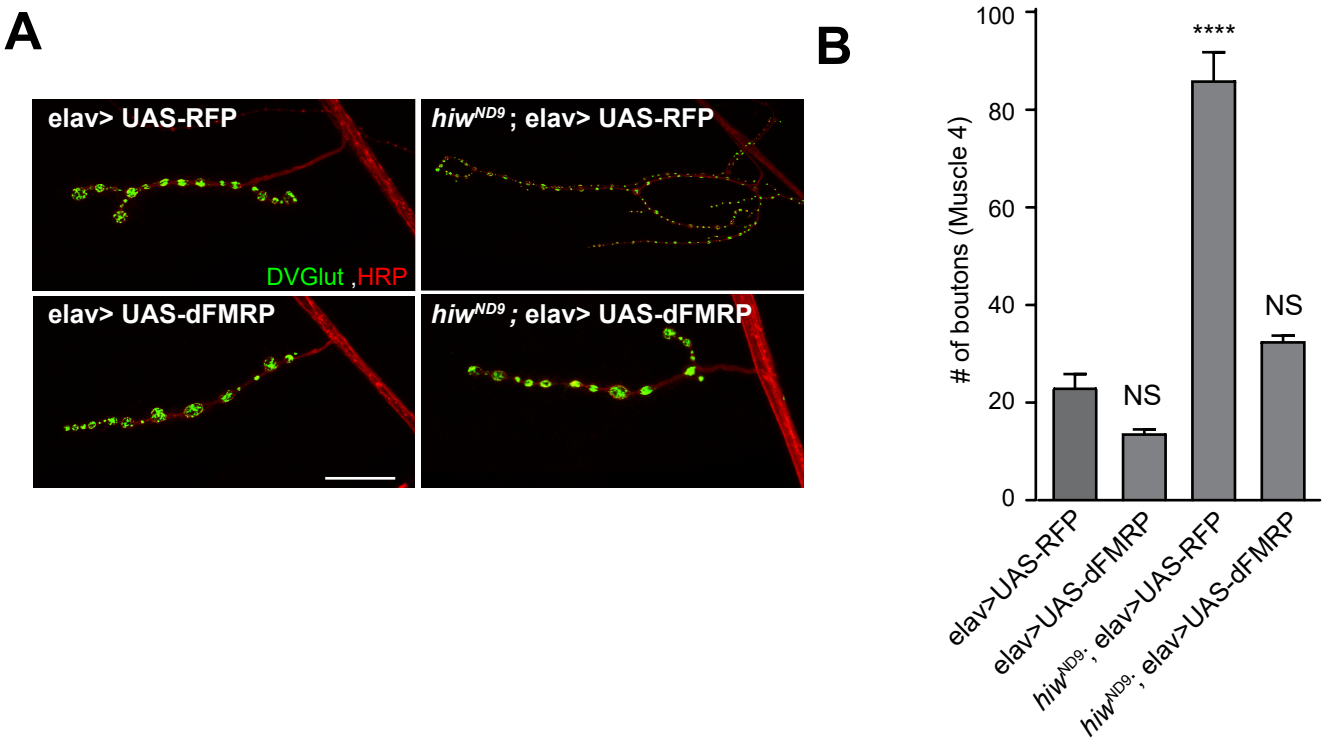

Figure S1, Related to Figure 1. Excess dFMRP does not alter NMJ growth in otherwise WT larvae, and suppresses overgrowth in a second *hiw* mutant background. (A) Representative images of the NMJ synaptic terminal at muscle 4 in third-instar larvae. For all genotypes, the pan-neuronal driver Elav-GAL4 was used to express the given transgene. NMJs were stained for the presynaptic bouton marker DVGLUT (green) and nerve membrane marker HRP (red). (B) Quantification of the mean (±SEM) number of DVGlut+ boutons per muscle 4 NMJ in each genotype, with each synaptic terminal contributing an n of 1. Overgrowth in this *hiw* allele was suppressed by dFMRP-overexpression, while dFMRP overexpression has no impact on basal NMJ growth. Statistical tests and exact p-values reported in Table S1. Scale bar = 25 µm. For all quantifications: * p= 0.05; ** p= 0.01; *** p = 0.001; **** p =0.0001, NS = not significant, p>0.05.

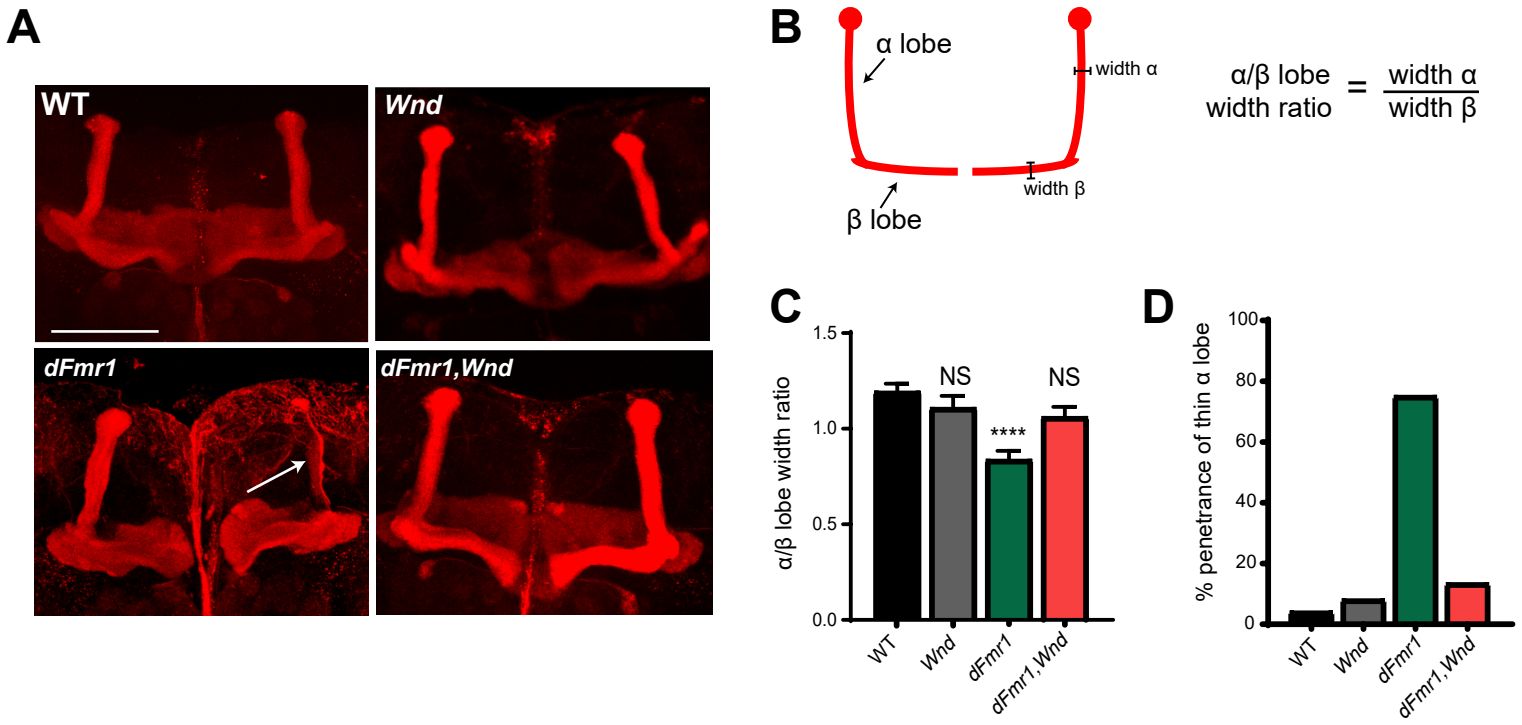

Figure S2, Related to Figure 3. Morphological abnormalities in *dFmr1* mushroom bodies are also Wnd-dependent. (A) Representative images of Drosophila mushroom bodies from WT, *Wnd* mutants, *dFmr1* mutants, and *Wnd,dFmr1* double mutants. Exact genotypes in **Table S1**. Antibody against Fasciclin II (FasII, Red) was used to label and visualize the α and β lobes of the mushroom bodies. The representative image for *dFmr1* illustrates a severe case of the thin α lobe phenotype (white arrow), which was the most prominent and common phenotype observed. (B) Schematic depicting α and β lobe projections and the measurements taken to define the α/β lobe width ratio for each mushroom body. (C) Quantification of the α/β lobe width ratio for all four genotypes. (D) Penetrance of the thin α lobe phenotype in each genotype. A thin α-lobe was defined as an α-lobe in which the absolute width (measured in microns) was two standard-deviations less than the mean α-lobe width for WT mushroom bodies. The total number of α-lobes that met this criterion were counted per genotype, and thus the penetrance of this phenotype is represented here. Scale bar = 50 μm.

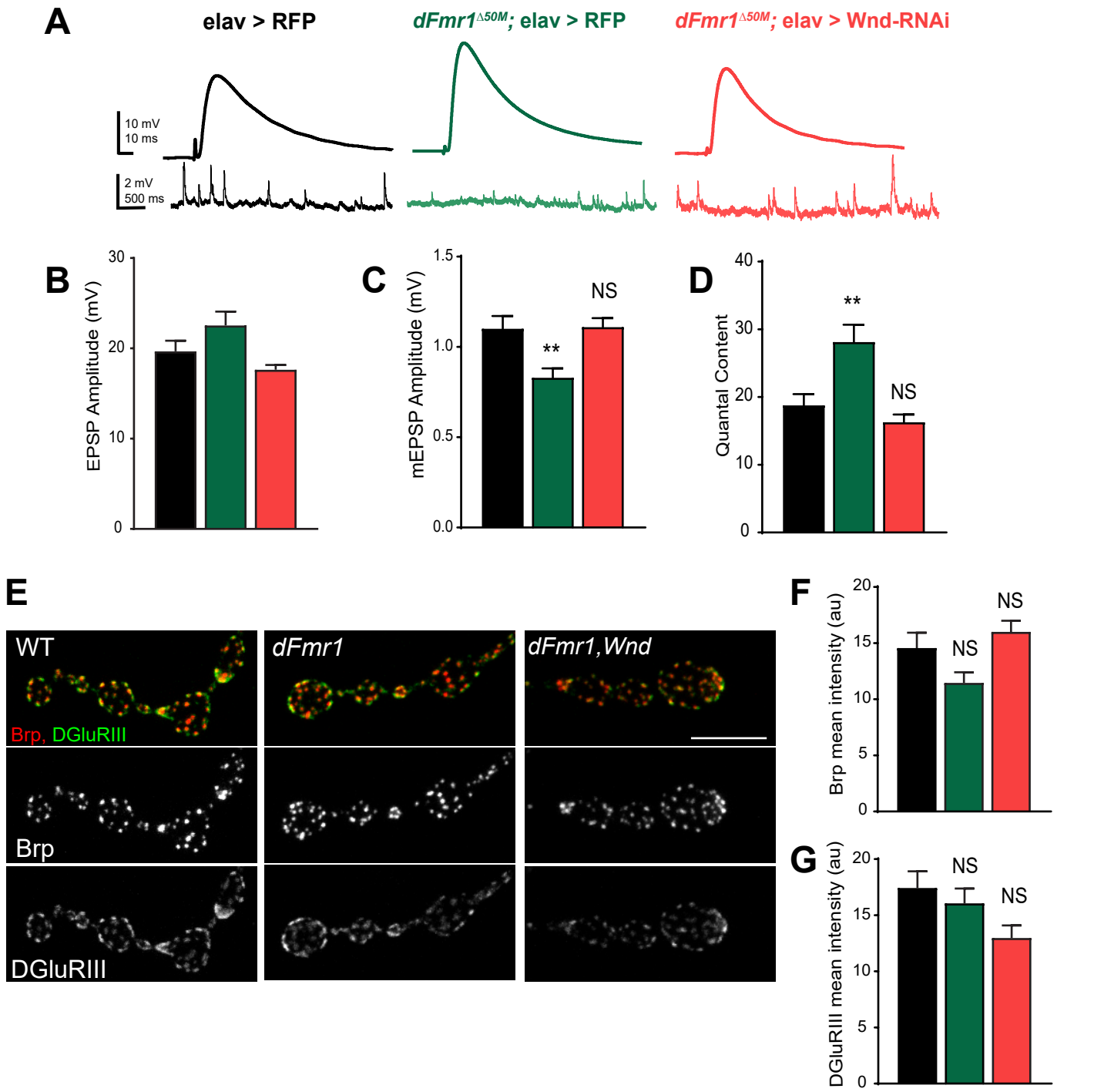

Figure S3, Related to Figure 4. Presynaptic Wnd drives abnormal synaptic transmission in *dFmr1* mutants, but active zone formation at *dFmr1* NMJs is grossly normal. (A) Representative EPSP and mEPSP electrophysiological traces from larval NMJs at Muscle 6. The pan-neuronal driver Elav was used to drive the control transgene UAS-RFP in either a WT background (elav > RFP), the *dFmr1* mutant background (*dFmr1*$^{\Delta 50M}$, elav>RFP), and we then knocked down Wnd by driving the Wnd-RNAi in the *dFmr1*$^{\Delta 50M}$, mutant background (*dFmr1*$^{\Delta 50M}$, elav>Wnd-RNAi). (B) Quantification of mean (±SEM) EPSP amplitudes, in which 75 consecutive evoked events were averaged per cell, and then cell amplitudes were averaged per genotype. (C) Quantification of mean (±SEM) mEPSP amplitudes, in which 75 consecutive spontaneous events were averaged per cell, and then cell amplitudes were averaged per genotype. (D) Quantification of quantal content, which was calculated individually per cell by dividing the mean EPSP amplitude by the mean mEPSP amplitude, and then averaged per genotype. This demonstrates that presynaptic Wnd is necessary for changes in synaptic transmission at the *dFmr1* mutant NMJ. (E) Representative images of WT, *dFmr1*, and *dFmr1,Wnd* NMJ boutons stained for the presynaptic scaffolding protein Brp (red) and the essential glutamate receptor subunits DGluRIII (also known as DGluRIIC - green). We did not observe differences in Brp or DGluRIII intensities in any genotype, nor were any apposition defects apparent, showing that synapse formation is largely intact in the absence of dFMRP. (F) Quantification of mean (±SEM) Brp intensity at the NMJ. (G) Quantification of mean (±SEM) DGluRIII intensity at the NMJ. Statistical tests and exact p-values reported in Table S1. For physiology, each cell recorded contributed an n of 1. For IHC, each NMJ terminal contributed an n of 1. Scale bar = 10 μm * p= 0.05; ** p= 0.01; *** p = 0.001; **** p =0.0001, NS = not significant, p>0.05.